AD_____

TECHNICAL REPORT
69-51-OSD

APPROXIMATE ANALYSIS OF A FLAT, CIRCULAR PARACHUTE IN STEADY DESCENT

by

Edward W. Ross, Jr.

December 1968

Office of the Scientific Director
U.S. ARMY NATICK LABORATORIES
Natick, Massachusetts

FOREWORD

Despite the fact that parachutes have been in use for many years, no completely satisfactory theory exists for the prediction of stresses in a canopy. This hinders good design. This report describes a mathematical model for predicting canopy shape and stresses in steady descent which is superior to those now in use. This model is embodied in a computer program that can be used for design studies if desired.

TABLE OF CONTENTS

ABSTRACT

A theory is presented for the stress analysis of a flat, circular parachute in steady, vertical descent. Unlike previous treatments of the problem, this theory does not assume that the shape is known. Instead, the theory presents relations between the pressure distribution in the opened condition and the shape, drag and stresses in lines and fabric. The theory results in a non-linear third order system of ordinary differential equations with boundary conditions at both vent and skirt. This system was solved by a computer program based on the Runge-Kutta method of numerical integration. The results are in fairly good agreement with measurements on parachutes. The computer program can be used for studies of effects of design changes on shape, drag and stress, and the results of a small study of this sort are included.

1. INTRODUCTION

In recent years repeated attempts have been made to analyze the behavior of parachutes and devise formulas suitable for their design. Much progress has been made, but the state of knowledge is still not wholly satisfactory. The best analyses currently available, Heinrich and Jamison[1] and Topping, Marketos and Costakos[2] rely on knowing the deformed shape as well as the pressure distribution before the stresses are analyzed even in steady descent. Present knowledge about large deflections of structures suggests that it should be possible to calculate the stresses and deformed shape concurrently, although some assumptions must still be made about the pressure distribution in the deformed state. We shall undertake to do this in the present paper.

To be specific, we analyze a flat circular parachute in steady, vertical descent by an approximate theory for large elastic deflections. This theory is like (but goes beyond) that of Heinrich and Jamison[1]. The parachute is regarded as a completely flexible structure, i. e., none of its elements (cloth, cords, reinforcing tape, etc) have any bending stiffness. The resulting analysis resembles the large-deflection (non-linear) membrane version of thin shell theory but differs from it because of the important part played by the cords. A number of assumptions are made, of which the most important are listed below:

(i) The strains in the fabric and cords are small even though the deflections are large.

(ii) The fabric is supposed to possess no resistance to stresses in the meridional (radial) direction, all forces in this direction being resisted solely by the cords.

(iii) Corresponding points on each gore experience identical stresses and deformations, and the same is true for each cord, i. e., the deformation is, loosely speaking, axially-axisymmetric.

(iv) The circumferential radius of curvature of the gores is everywhere much smaller than the meridional radius of curvature.

(v) For each gore points on a circular arc about the axis of the undeformed parachute lie in a plane perpendicular to the cords after deformation.

The analysis, which is described in the next Section, leads to a non-linear third-order system of ordinary differential equations, which cannot be integrated in closed form. Therefore a computer program was written for the solution of the system, based on the Runge-Kutta method of numerical integration. The program is automatic enough so that it is convenient to study the effect on the deformations, stresses, drag and parachute weight of any two, arbitrarily chosen, design parameters, such as the vertical velocity, number of gores or elastic moduli of various structural elements. A description

of the program is given in Section 3 , and examples of the results obtained are displayed in Section 4. Section 5 contains a discussion of the analysis and results.

2. ANALYSIS

In analyzing the parachute we first treat a generic one of the gores, which is assumed to be a flat sector of a circle in the undeformed state. If G is the number of gores, then the sectorial angle in both the undeformed and deformed states is

$$\alpha = 2\pi/G \tag{1}$$

We examine first the kinematics, then the statics and finally the material behavior of the fabric.

Kinematics: Let A and B denote the material points where a generic circular arc in the undeformed state meets the cords that border the gore. In the undeformed state this arc, $\overline{AB}$, has length, $R\alpha$; see Figure 1. We assume that after deformation the arc $\overline{AB}$ forms a plane circular arc, the plane of the arc being perpendicular to the deformed cords, Figure 2. The points A and B are now at a distance r from the axis and are separated by a distance r_α. If r_{AB} is the radius of this circular arc and 2β is the sectorial angle, then we see from Figure 3 that, provided $0 \leq \beta \leq \pi/2$,

$$r_{AB} \sin\beta = (1/2) r_\alpha \tag{2}$$

$$2\beta r_{AB} = \text{Deformed length of arc } \overline{AB} \tag{3}$$

If $\beta = \pi/2$, we may have a situation where adjacent gores are

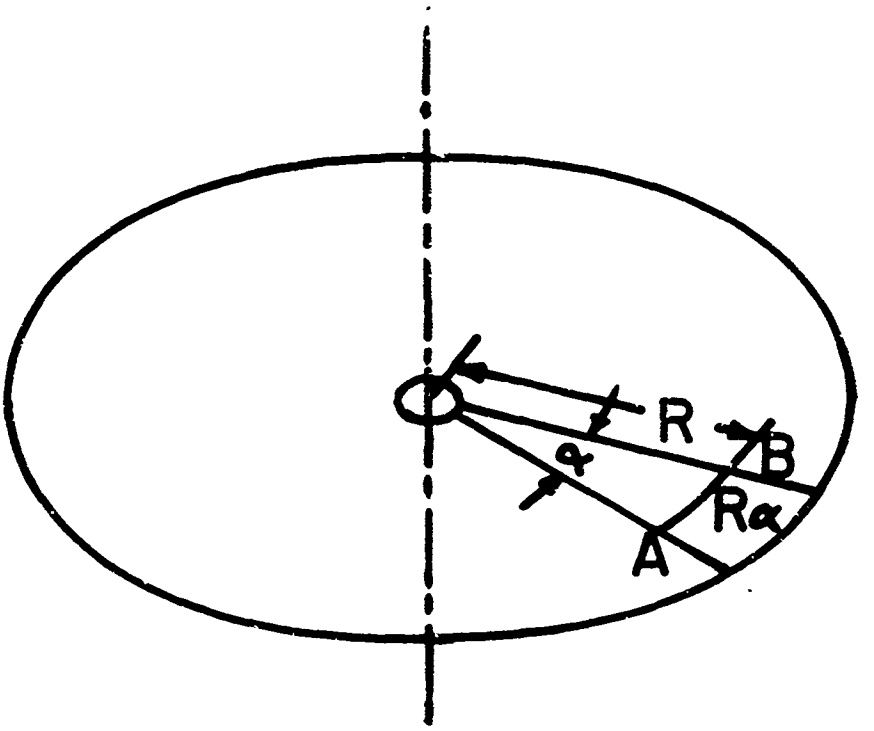

Figure 1: Undeformed parachute gore

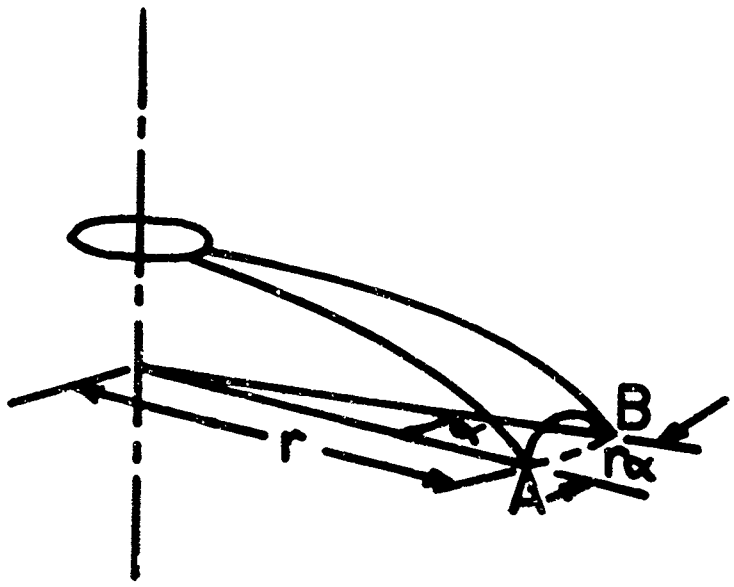

Figure 2: Deformed parachute gore

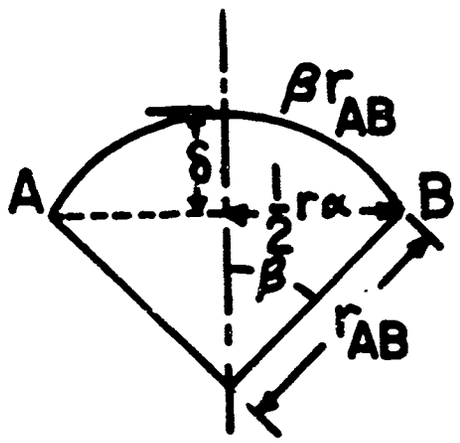

Figure 3: Section of deformed gore normal to cords, $\sigma'=0$

pressed against each other with a contact length σ' as shown in Figure 4.

In this case

$$r_{AB} = (\pi/2)r\alpha \tag{4}$$

$$\text{Deformed length of } \overline{AB} = 2\sigma'+\pi r_{AB}$$

$$= 2\sigma'+(\pi/2)r\alpha \tag{5}$$

The undeformed length of $\overline{AB}$ is $R\alpha$, so we may write formulas for the circumferential fabric strain, γ_f, which is assumed small,

γ_f = change in length/original length

$$\gamma_f = (2\beta r_{AB}/R\alpha) - 1 \quad \text{if } \beta<\pi/2 \tag{6}$$

$$\gamma_f = \{[2\sigma'+(\pi/2)r\alpha]/R\alpha\} - 1 \quad \text{if } \beta = \pi/2 \tag{7}$$

Statics: If N_f is the circumferential tension in the gore fabric, with dimensions (lbs/ft) and p is the pressure difference between the inside and outside of the surface, then equilibrium requires

$$N_f = pr_{AB} \tag{8}$$

The forces exerted by the fabric on the cords, per unit length of cord are shown in Figure 5. The forces in the circumferential and normal directions, N_θ and N_n, are found from conditions of equilibrium,

$$N_\theta = N_f \cos\beta \tag{9}$$

$$N_n = 2N_f \sin\beta \tag{10}$$

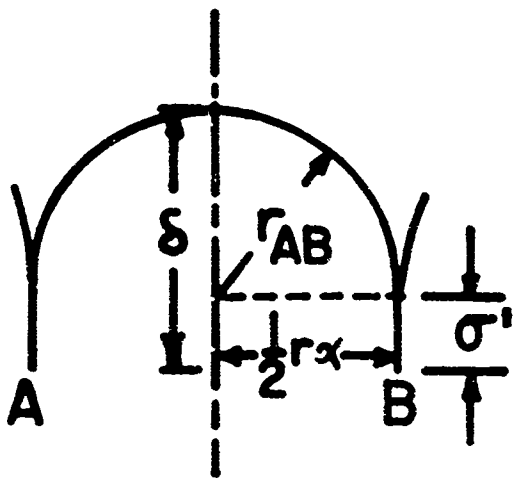

Figure 4: Section of deformed gore normal to cords, $\sigma' \neq 0$

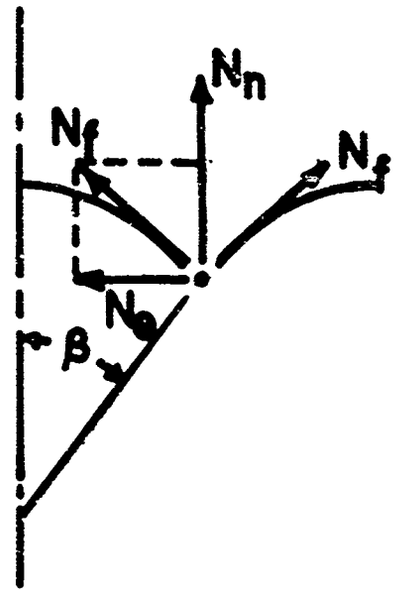

Figure 5: Forces transmitted from gore fabric to cords

If we use (2) and (8), we obtain for $\beta \neq 0$

$$N_\theta = (1/2)pr\alpha \cot \beta \tag{11}$$

$$N_n = pr\alpha \tag{12}$$

These formulas are valid both for $\beta<\pi/2$ and $\beta = \pi/2$, and in the latter case they imply

$$N_\theta = 0.$$

Material Behavior: We assume that the fabric obeys a linear elastic law,

$$N_f = E_f\gamma_f \tag{13}$$

where E_f is the elastic constant of the fabric when stressed in the circumferential direction. If $\beta<\pi/2$, we may use (2), (6) and (8) to rewrite this relation in the form

$$r/R = \beta^{-1}\{\sin\beta+(1/2)(p/E_f)r\alpha\} \tag{14}$$

This can also be written, with the aid of (11) as

$$r/R = \beta^{-1}\sin\beta\{1+(N_\theta/E_f)\sec\beta\},$$

or

$$N_\theta/E_f = \cos\beta\{\beta \csc\beta\,(r/R) -1\} \tag{15}$$

We see from (15) that in the limit as $\beta \to 0$ we obtain

$$N_\theta/E_f \to (r/R) -1.$$

This can be interpreted to mean that, when the fabric is stretched flat between the cords, i. e., when there is negligible bulging of the gores, we recover the linear elastic relation between circumferential stress resultant and circumferential strain.

In the calculations we shall adopt (15) together with formulas equivalent to (14) and (13)

$$\sin\beta - \beta(r/R)+(1/2)(p/E_f)r\alpha = 0 \tag{16}$$

$$N_f = E_f\{\beta\csc\beta(r/R) - 1\} \tag{17}$$

as expressing the material behavior of the fabric when $\beta<\pi/2$.

When $\beta = \pi/2$, the elastic law (13) implies

$$(1/2)(p/E_f)r\alpha = \{[2\sigma'+(\pi/2)r\alpha]/R\alpha\} - 1$$

or

$$\sigma' = (1/2)R\alpha\{1 -(\pi/2)(r/R)+(1/2)(p/E_f)r\alpha\} \tag{18}$$

together with

$$N_\theta = 0 \tag{19}$$

$$N_f = (1/2)pr\alpha \tag{20}$$

We have now completed the portion of the analysis that deals with the fabric.

In analyzing the fabric we have neglected the meridional stresses on the assumption that stresses of this type are borne entirely by the cords. We must now, therefore, analyze the statics and material behavior of the cords.

Statics of Cords: If N_c is the tension force in the cords, measured in lbs, then we can write down the two equations of force equilibrium in the direction tangential and normal to the cords with the aid of Figures 6 and 7. These are

$$dN_c/ds = 2N_\theta\sin(\alpha/2)\cos\phi \tag{21}$$

$$\begin{aligned} N_c d\phi/ds &= N_n - 2N_\theta\sin(\alpha/2)\sin\phi \\ &= pr\alpha - 2N_\theta\sin(\alpha/2)\sin\phi \end{aligned} \tag{22}$$

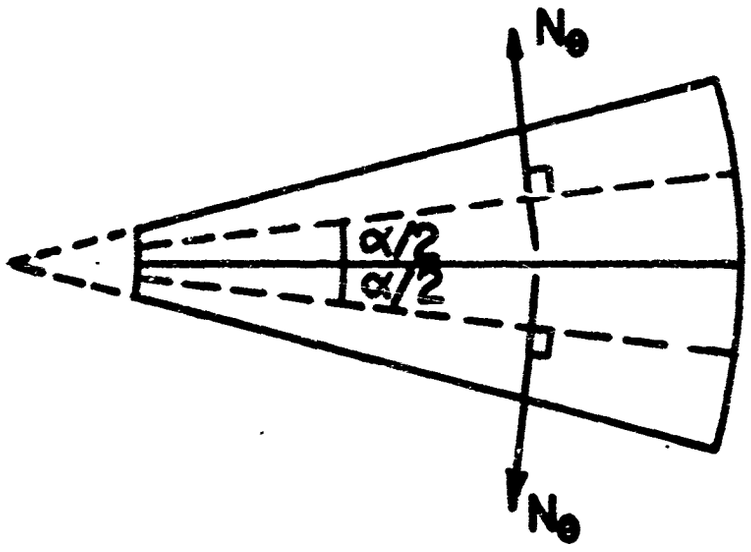

Figure 6: Sketch showing that the resultant of the N_θ forces on a cord is a radial inward force, $2r_a \sin(\alpha/2)$ per unit of cord length

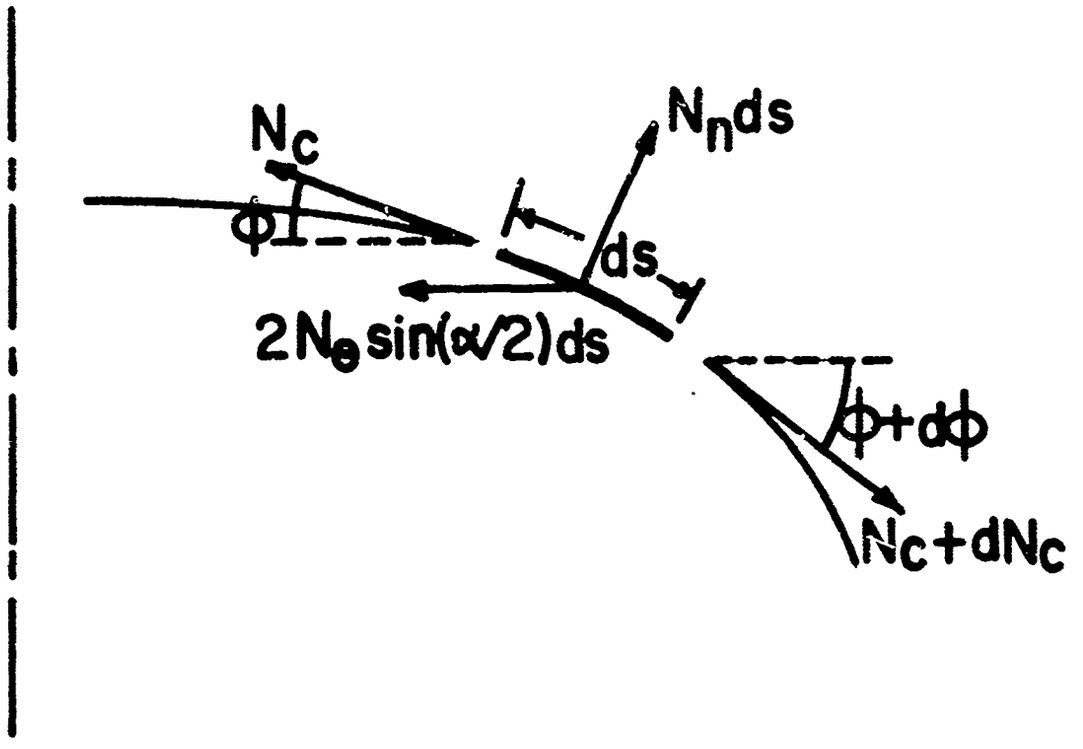

Figure 7: Forces acting on an element of cord with length ds

A partial check on the validity of these equations is provided by studying their behavior as $\alpha \to 0$. If we set $N_c = \alpha N_s$, these should reduce to the equations of equilibrium of membrane shell theory,

$$d(rN_s)/dr = N_\theta \tag{23}$$

$$N_s\, d(\sin\phi)/dr + N_\theta(\sin\phi/r) = p. \tag{24}$$

If we use the fact that (see Figure 8)

$$dr = ds\cos\phi, \tag{25}$$

and observe that

$$(2/\alpha)\sin(\alpha/2) \to 1$$

as $\alpha \to 0$, we see that equations (21) and (22) reduce to the proper limit as $\alpha \to 0$.

Material Behavior of Cords: The strain in the cords, γ_s, is assumed to be small and we infer from Figure 9 that

$$\gamma_s = (ds-dR)/dR = (dr/dR)\sec\phi - 1$$

The cords are assumed to obey a linear elastic relation

$$N_c = E_c\gamma_s = E_c\{(dr/dR)\sec\phi - 1\}. \tag{26}$$

This completes the analysis of the cords.

To put these equations into systematic form we observe that

$$dr/dR = \{1+(N_c/E_c)\}\cos\phi = f\cos\phi \tag{27}$$

where

$$f = 1+(N_c/E_c).$$

Since

$$d/ds = (dr/ds)(d/dr) = (dr/ds)(dR/dr)(d/dR)$$

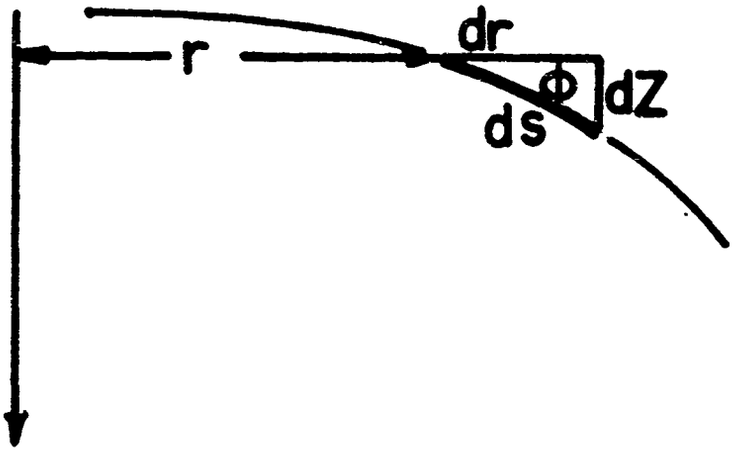

Figure 8: Geometry of deformed cord

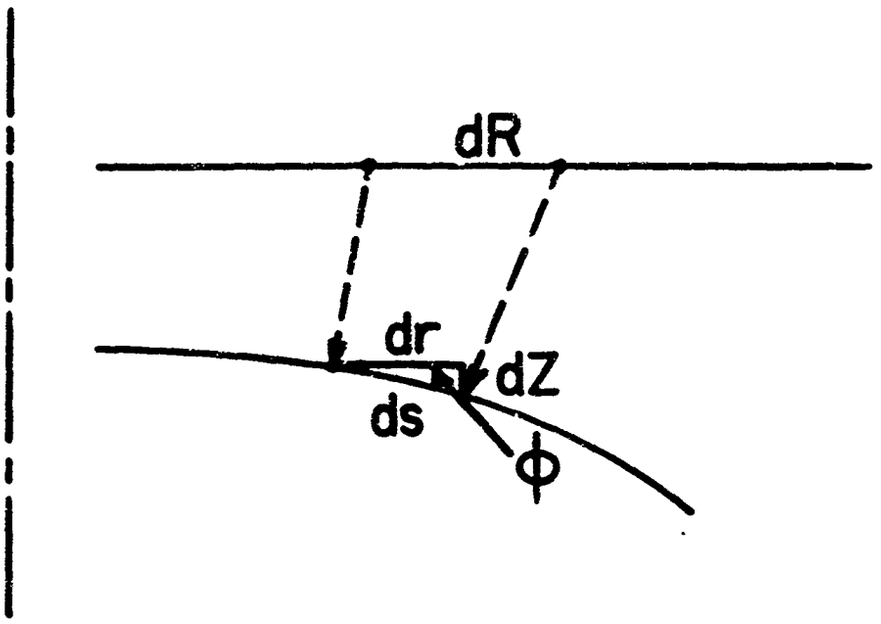

Figure 9: Derivation of formula for strain in cord

we find from (25) and (27) that

$$d/ds = (1/f)\,(d/dR).$$

Thus the equations of equilibrium and elasticity for the cords form the system

$$dr/dR = f\cos\phi \tag{28}$$

$$d\phi/dR = (f/N_c)\{pr\alpha - 2N_\theta \sin(\alpha/2)\sin\phi\} \tag{29}$$

$$dN_c/dR = 2fN_\theta \sin(\alpha/2)\cos\phi \tag{30}$$

where

$$f = 1+(N_c/E_c) \tag{31}$$

and N_θ is determined as follows. If

$$1+(r/2)\{(p\alpha/E_f)-(\pi/R)\} \leq 0$$

then

$$N_\theta = \alpha_f \cos\beta\{(r/R)\beta\csc\beta - 1\} \tag{32}$$

where β is found by solving the transcendental equation

$$\sin\beta - \beta(r/R)+(pr\alpha/2E_f) = 0 \tag{33}$$

If

$$1+(r/2)\{(p\alpha/E_f) - (\pi/R)\} > 0$$

then

$$N_\theta = 0 \tag{34}$$

$$\sigma' = (R\alpha/2)\{1+(pr\alpha/2E_f) - (\pi r/2R)\}$$

This is a third order, non-linear differential equation system in the three unknowns r, ϕ and N_c, and therefore we shall need three edge conditions in order to have a unique solution. At the vent, $r = r_1$ or $R = R_1$,

the cords continue across to the opposite side of the vent through the axis of symmetry (see Figure 10). The elastic law for the cords implies that

$$r_i = R_i + \{(N_c(R_i)/E_c\} \tag{35}$$

We shall take for another condition at the vent

$$\phi = 0. \tag{36}$$

These conditions are satisfied with good accuracy in a flat circular canopy although in other kinds of parachutes, notably those with the pull-down vent, more complicated conditions must be imposed.

The third condition is at the skirt, $r = r_o$ or $R = R_o$. From the geometry, see Figure 11, we obtain

$$r_o - L \cos(\pi - \phi_o) = r_o + L \cos\phi_o = 0 \tag{37}$$

where L is the deformed length of the suspension lines between the skirt and the load (or confluence point). If L_o is the undeformed length of the suspension lines, and γ_L is the strain in the suspension lines (which we do not assume small), then

$$L = L_o(1+2\gamma_L)^{1/2}$$

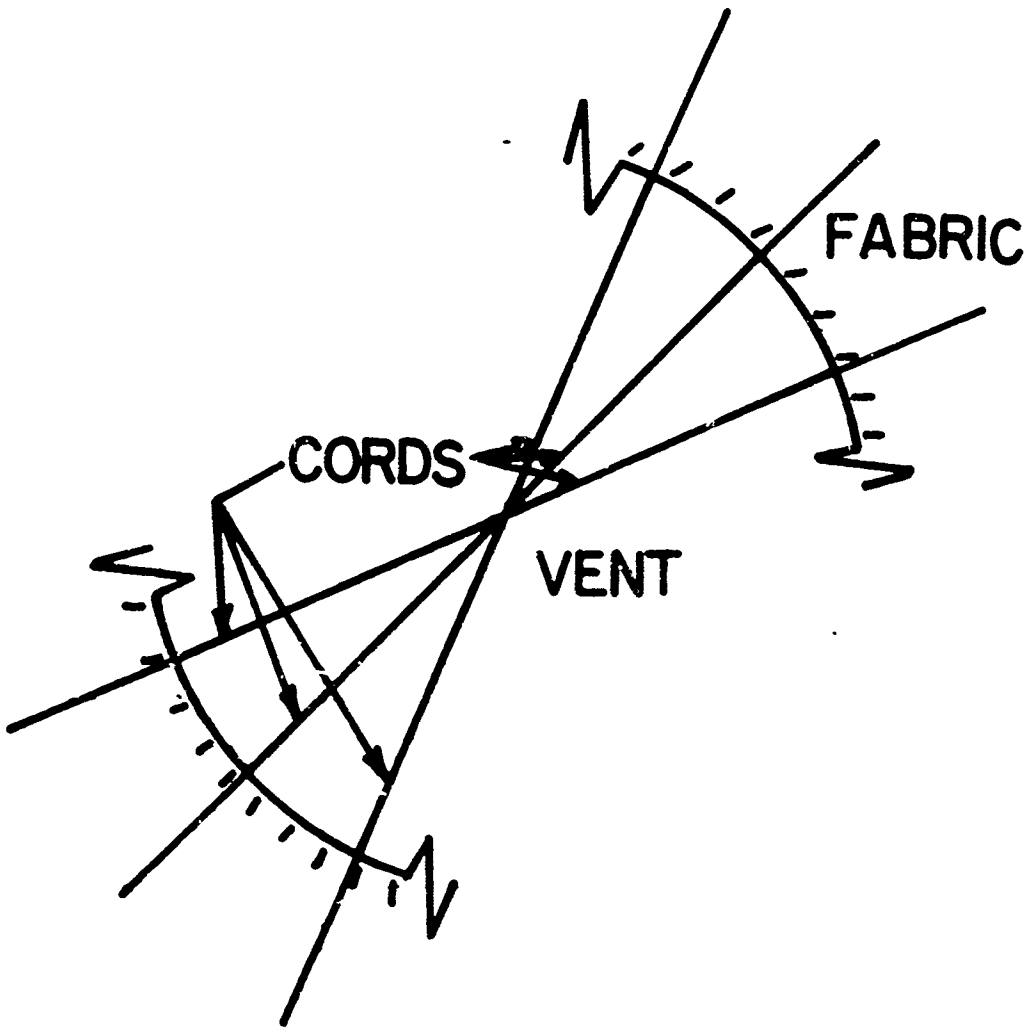

Figure 10: Sketch of the vent

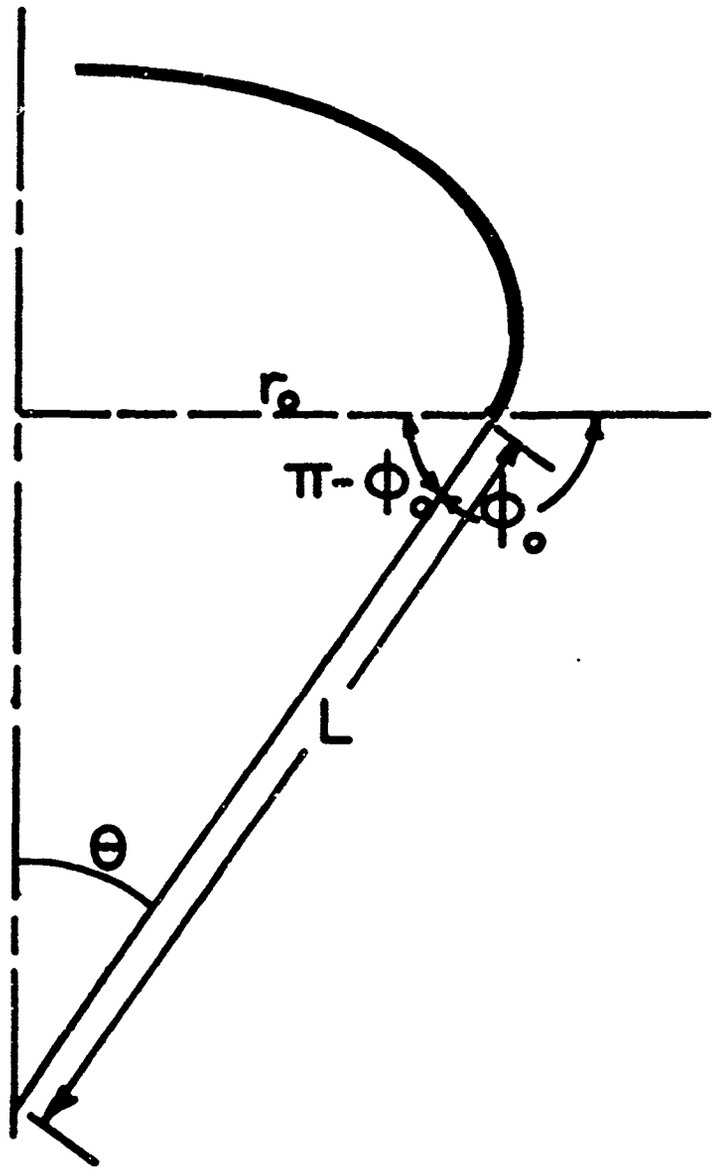

Figure 11: Geometry of skirt and load lines

The tension force in the lines is simply $N_c(R_o)$, the tension force in the cords at the skirt, hence, if E_L is the elastic modulus (lbs) of the lines,

$$\gamma_L = N_c(R_o)/E_L$$

$$L = L_o\left[1+\left(2N_c(R_o)/E_L\right)\right]^{1/2}$$

Then from (37) we find the condition which has to be satisfied at the skirt,

$$r(R_o)+L_o\left\{1+\left[2N_c(R_o)/E_L\right]\right\}^{1/2}\cos\phi(R_o) = 0 \qquad (38)$$

We have therefore reduced the problem of finding the deformed shape and stresses in the parachute to that of solving the system of three, non-linear, ordinary differential equations (28) - (30) for r(R) and $\phi(R)$ and $N_c(R)$. The quantities f and N_θ, which occur in the right sides of (28) - (30), are determined as functions of N_c, r and R by means of (31) - (34). The edge conditions on the differential equation system are (35), (36) and (38).

When this system has been solved, the drag, or weight of the load, can be found from

$$D = GN_c(R_o)\sin\phi(R_o) \qquad (39)$$

Also the deformed shape is found by calculating the cord profile, r(R) and Z(R), and the gore centerline profile, $r_g(R)$ and $Z_g(R)$, see Figure 12. In this calculation r(R) is of course known directly from the differential equation solution, but Z(R) must be found by integrating

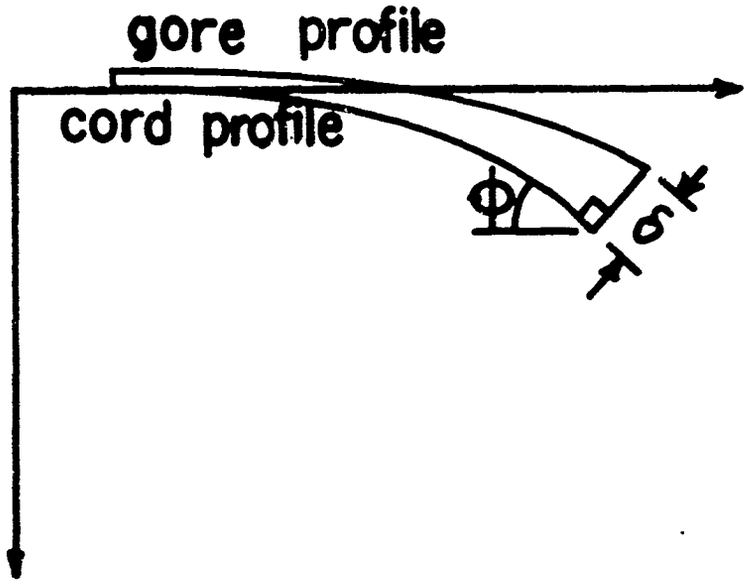

Figure 12: Profiles of deformed cord and gore centerline

$$dZ = dr \tan\phi = (dr/dR)\, dR \tan\phi$$

and so we find with the aid of (28)

$$Z = \int_{R'=0}^{R} f(R')\sin\phi(R')dR'$$

$$Z = \int_{R'=0}^{R} \{1+(N_c(R')/E_c\}\sin\phi(R')dR'. \qquad (40)$$

The gore centerline profile is then found, as in Figure 12,

$$r_g = r+\delta\sin\phi \qquad (41)$$

$$Z_g = Z-\delta\cos\phi \qquad (42)$$

where δ, the depth of centerline bulging, is given by different formulas for $\sigma' = 0$ and $\sigma'>0$. If $\sigma' = 0$, $\beta<\pi/2$ and (see Figure 3)

$$\delta = r_{AB}(1-\cos\beta) = (1/2)\, r\alpha(1-\cos\beta)/\sin\beta$$

$$= (1/2)r\alpha\tan(\beta/2) \qquad (43)$$

If $\sigma'>0$, $\beta = \pi/2$, we find from Figure 4

$$\delta = (1/2)\, r\alpha+\sigma'. \qquad (44)$$

We shall now re-phrase this entire system of equations in dimensionless form by introducing the new definitions

$$\begin{array}{llll} R = xR_i, & r = yR_i & L_o = JR_i, & R_o = x_oR_i, \\ N_c = E_cn_s, & N_\theta = E_fn_c, & N_f = E_fn_f, & Z_g = z_gR_i, \\ p = q\cdot 2E_f/R_i, & U_f = E_fR_i/E_c, & U_L = E_L/E_c, & r_g = y_gR_i, \\ D = E_cW, & \sigma' = \sigma R_i, & Z = zR_i, & \delta = \Delta R_i \end{array} \qquad (45)$$

The equations become

$$dy/dx = f\cos\phi \tag{46}$$

$$d\phi/dx = (2U_f f/n_s)\{q\alpha y - n_c \sin(\alpha/2)\sin\phi\} \tag{47}$$

$$dn_s/dx = 2fU_f n_c \sin(\alpha/2)\cos\phi \tag{48}$$

$$f = 1+n_s \tag{49}$$

If

$$1+q\alpha y-[\pi y/(2x)]<0$$

then

$$n_c = \cos\beta\{\beta(y/x)\csc\beta - 1\} \tag{50}$$

where β satisfies

$$\sin\beta - \beta y/x - q\alpha y = 0 \tag{51}$$

and if

$$1+q\alpha y-(\pi y/2x)\geq 0$$

then

$$n_c = 0, \quad \beta=\pi/2 \tag{52}$$

$$\sigma = (1/2)x\alpha\{1+q\alpha y-(\pi y/2x)\} \tag{53}$$

the edge conditions are

$$n_s(1) = y(1)-1 \tag{54}$$

$$\phi(1) = 0 \tag{55}$$

$$y(x_o)+J\{1+[2n_s(x_o)/U_L]\}^{1/2}\cos\phi(x_o) = 0 \tag{56}$$

The dimensionless load or drag is

$$W = Gn_s(x_o)\sin\phi(x_o), \tag{57}$$

$$z(x) = \int_o^x \{1+n_s(x')\}\sin\phi(x')dx' \qquad (58)$$

$$y_g = y+\Delta\sin\phi \qquad (59)$$

$$z_g = z-\Delta\cos\phi \qquad (60)$$

and

$$\Delta = (1/2)y\alpha\tan(\beta/2) \quad \text{if } \beta<\pi/2 \qquad (61)$$

$$\Delta = \sigma+(1/2)y\alpha \quad \text{if } \beta = \pi/2 \qquad (62)$$

In discussing the pressure and stress distributions it is also convenient to define dimensionless stress, drag and pressure coefficients in a manner different from the dimensionless quantities previously defined*. We shall take

$C_p = p/\{(1/2)\rho V^2\}$ = pressure coefficient

$C_{Do} = D/\{(1/2)\rho V^2\pi R_o^2\}$ = drag coefficient

$C_c = N_c/\{(1/2)\rho V^2\pi R_o^2\}$ = cord stress coefficient

$C_f = N_f R_o/\{(1/2)\rho V^2\pi R_o^2\}$ = fabric stress coefficient

If the foregoing analysis is correct, we must satisfy the 3rd order differential equation system (46) - (49) together with the auxiliary equation (50) - (53) and the edge condition (54) - (56). This system was taken as the basis for the computer program. The numerical analysis underlying the computer program is described in the next Section.

---

*Notice that because of (13), (26) and (35) the dimensionless stresses n_f and n_s, defined in (45), are also respectively just the strains γ_f, γ_s.

3. NUMERICAL ANALYSIS OF THE PROBLEM

The numerical analysis of this problem consists primarily of solving the differential equation system (46) - (48) by numerical means and secondarily satisfying the edge conditions. We shall deal below with these two aspects of the problem and then describe other aspects of the computer program.

The treatment of the differential equation system is based on the well-known Runge-Kutta method for numerical integration. The procedure is not quite routine because of the need to evaluate n_c and insert it in the right side of (47) and (48) at each step, n_c being determined by (50) - (52). In particular, if

$$1+q_\alpha y-\{\pi y/(2x)\}<0,$$

we must determine β by solving (51) and then evaluating t_c from (50). The solution of (51) was accomplished by using the Newton - Raphson iteration defined by

$$\beta_{k+1} = \beta_k - \left\{\frac{q_\alpha y+\sin\beta-\beta(y/x)}{\cos\beta - (y/x)}\right\} \qquad (66)$$

As usual with this procedure convergence is uncertain. However, it became clear after a little study that convergence occurred when the initial β was chosen well above the value of β for which

$$\cos\beta = y/x.$$

This condition was satisfied by choosing as starting values

$$\beta = .4 \text{ if } \varepsilon\geq 0$$

$$\beta = .4+(-2\varepsilon)^{1/2} \text{ if } \varepsilon<0.$$

$$\varepsilon = (y/x)-1.$$

In order to avoid difficulties for small values of β in (50), explicit polynomial approximations were used for the trigonometric function, i. e.,

$$\cos \beta \simeq 1-C_1\beta^2+C_2\beta^4$$

$$\sin \beta \simeq \beta(1-S_1\beta^2+S_2\beta^4)$$

C_1, C_2, S_1, S_2 constants

With these approximations we may write (66) and (50) as

$$\beta_{k+1} \simeq \beta_k+\left\{\frac{q\alpha y-\beta[\varepsilon+\beta^2(S_1-S_2\beta^2)]}{\varepsilon+\beta^2(C_1-C_2\beta^2)}\right\} \equiv \beta_k - H_k \quad (67)$$

$$n_c \simeq \frac{\{\varepsilon+\beta^2(S_1-S_2\beta^2)\}}{\{1-\beta^2(S_1-S_2\beta^2)\}} \{1-C_1\beta^2+C_2\beta^4\} \quad (68)$$

These formulas are sufficiently accurate for practical purposes and are well-behaved for $0 \leq \beta \leq \pi/2$.

Because the edge conditions (54) - (56) are not all applied at the same point, it is necessary to adopt a trial-and-error scheme in order to satisfy them. This is begun by assuming a value for the deformed vent radius, y(1). Next the values of $n_s(1)$ and $\phi(1)$ are found from (54) and (55), n_c (1) is evaluated as in the preceding paragraph and we can then begin the Runge-Kutta procedure for integrating the differential equation system. With this procedure the solution is built out in the x-direction until the values at the skirt, $y(x_o)$, $\phi(x_o)$ and $n_s(x_o)$ are obtained.

These values should satisfy (56). Usually, of course, they will not, and we must change the assumed value of y(1) and start again. In the program this process is made automatic by including a subroutine that applies the Rule of False Position when a sign change is found in the left side of (56).

In the program a general pressure distribution is assumed, given by

$$C_p = A_o + A_1\phi + A_2\phi^2 + A_3\phi^3 \qquad (69)$$

The constants A_o, A_1, A_2 and A_3 are read in and permit a fairly wide choice of pressure distributions. The scarcity of reliable information on pressure distributions makes this procedure necessary. It is worth noticing that C_p is assumed to be a function of ϕ (the deformed cord angle) and so depends to a certain extent on the deformed shape.

After finding the complete solution, satisfying all the edge conditions, the program carries out the numerical integration of (58), using Simpson's Rule, and calculates the cylindrical coordinates of the cord and gore centerlines by means of (59) - (62).

In order to make the program useful for design purposes, provision is made for the computation of certain information beyond merely the shape and stresses. This extra information includes an analysis of the parachute weight, i. e.,the distribution of the total weight among the different structural elements (fabric, cords, fixtures etc). Also the maximum

cord and fabric stresses, as well as the vent and load line stresses, are calculated and compared with the respective breaking stresses to find safety factors for each structural element. Warning messages are printed if the safety factors fall below unity.

The program is arranged so that in one pass the user may choose any two of the input quantities and vary these independently by chosen numbers of chosen increments, so that the effect on the solutions of changes in these quantities may be studied. For instance, the drop velocity, V, and fabric modulus, E_f, may be varied, or the effect of changing two constants in the hypothetical pressure distribution (69) may be found.

4. EXAMPLES OF RESULTS

This program was used to study the effects of different variables on the shape, drag and stresses. For this purpose a basic set of parameter values was chosen, typical of the C-9 canopy.

Vent radius = 1.4 ft

Ratio of skirt to vent radii = 10

No. of gores = 28

Suspension Line Length = 28 ft

Elastic Modulus of Cords = 2×10^3 lbs

Elastic Modulus of Fabric = 2×10^3 lbs/ft

Elastic Modulus of Load Lines = 2×10^3 lbs

The mass density of air was taken as

$$\rho = 2 \times 10^{-3} \text{ lb-sec/ft}^4.$$

and the drop velocity as

$$V = 20 \text{ ft/sec}$$

The basic pressure distribution was taken as a constant function $C_p = 1.5$, defined by

$$A_o = 1.5, \; A_1 = A_2 = A_3 = 0$$

For this basic configuration the following results were found:

C_{D_o} = Drag coefficient = .626

D_p = max. diameter = .671 D_o

ϕ_o = cord angle at skirt = 109^o

or

$\theta = \phi_o - (\pi/2) = 19^o$

where $D_o = 2R_o$ is the flat circular diameter and θ is the angle between the suspension lines and the canopy axis. The deformed shape is shown in Figure 13, and the cord and fabric stress coefficients are depicted in Figure 14.

The theory was further tested by investigating the influence of various parameters on the shape, drag and stresses. A large number of results was obtained, the most important of which are displayed in Tables 1 and 2. We may summarize the main features as follows:

(i) Table 1 shows that D_p/D_o, and hence the shape, is not greatly affected by any of the parameter changes. The suspension line length ratio, Λ, has the greatest effect on D_p/D_o, but its effect is not especially large.

(ii) According to Table 1, Λ is the only canopy parameter that affects the drag coefficient significantly. The effects of G and V are small, and the elastic constants have negligible influence.

(iii) The angle, θ, of the load lines, which is the same as the angle of the cords at the skirt, is seen in Table 1 to be significantly affected only by changes in Λ.

(iv) We conclude from Table 1 that G is the only variable that greatly influences $C_{c\ max}$ although Λ has some effect. In contrast $C_{f\ max}$ is perceptibly affected by changes in all the canopy parameters.

(v) The cord stress is least at the vent and increases to a maximum at the maximum diameter, which is usually at $x = 9$, i. e. near the skirt. Hence the familiar formula

$$C_c = C_{D_o}/G \cos \theta,$$

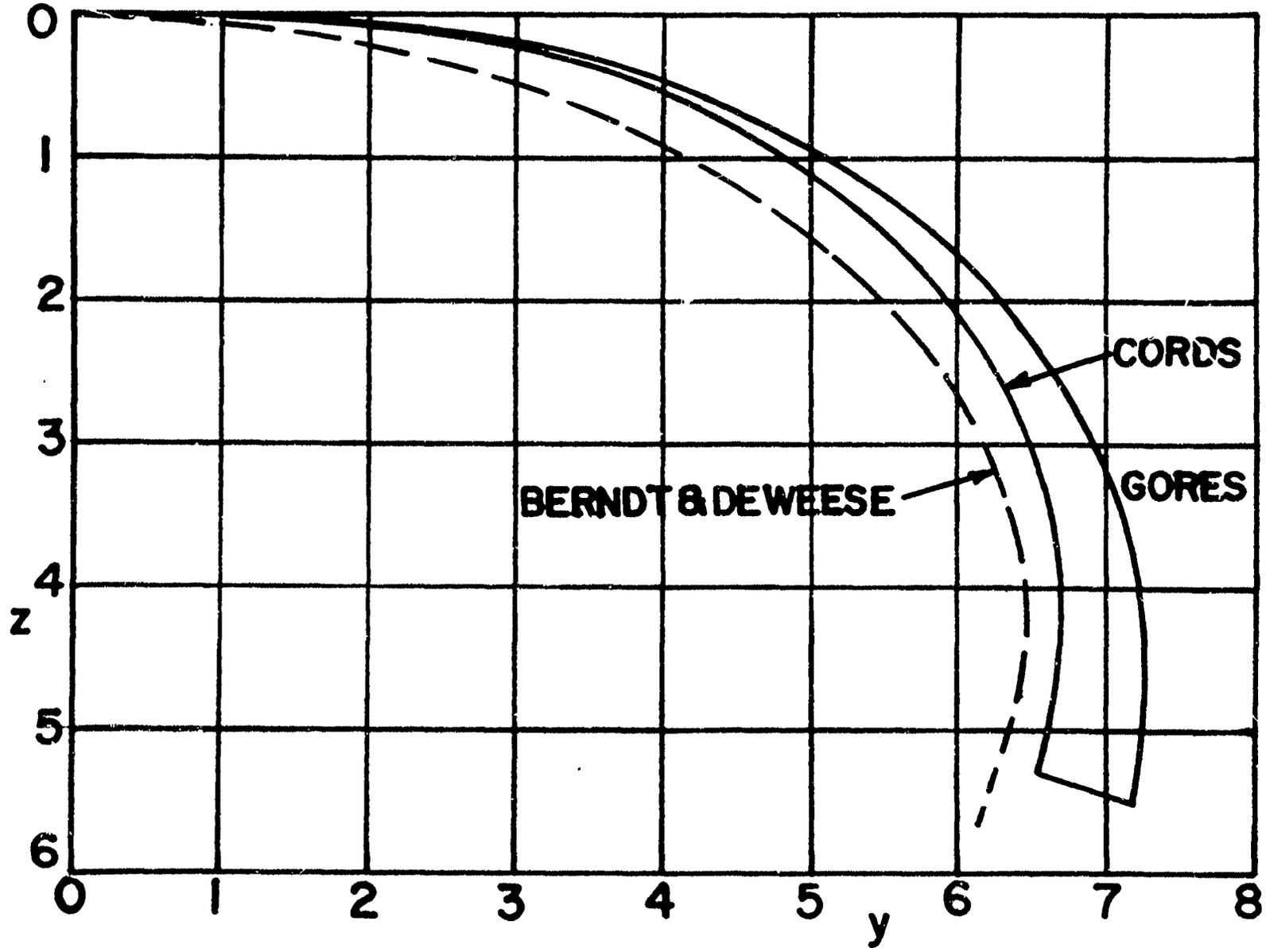

Figure 13: Deformed shape for basic configuration

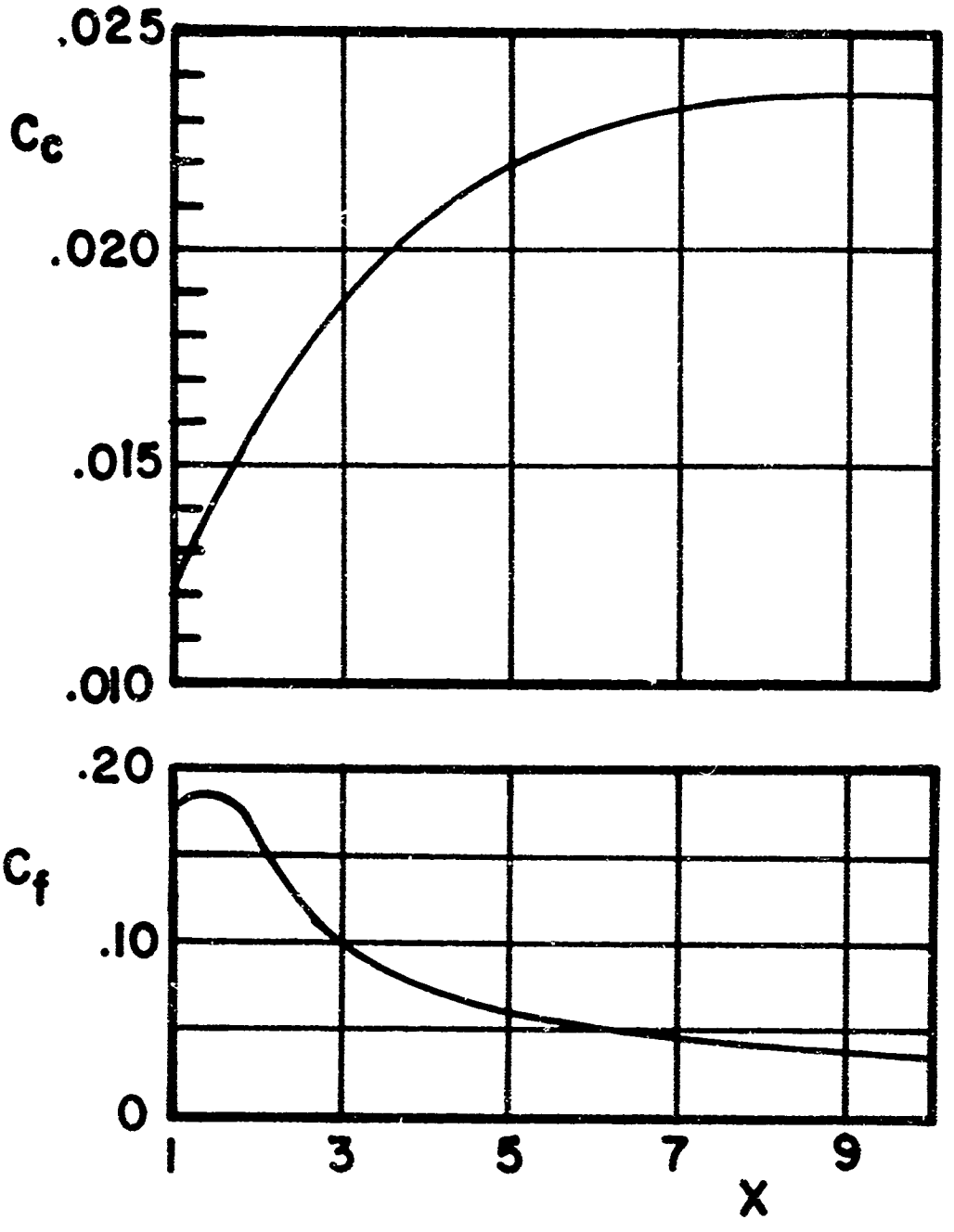

Figure 14: Cord and fabric stress coefficients for basic configuration

TABLE 1

Parameter	D_p/D_o	C_{D_o}	Max C_c	Max C_f	$\Theta = \phi_o - (\pi/2)$
E_c					
1000	.673	.627	.0237	.264	19°
2000*	.671	.626	.0237	.185	19°
3000	.671	.625	.0236	.155	19°
E_f					
400	.672	.626	.0237	.087	19°
1200	.672	.626	.0237	.140	19°
2000*	.671	.626	.0237	.185	19°
G					
16	.665	.614	.0406	.219	19°
28*	.671	.626	.0237	.185	19°
40	.674	.630	.0167	.155	19°
Λ					
.7	.645	.549	.0218	.175	26°
1.0*	.671	.626	.0237	.185	19°
1.3	.687	.671	.0248	.191	15°
V					
10	.670	.623	.0236	.210	19°
20*	.671	.626	.0237	.185	19°
30	.673	.629	.0238	.176	19°

*Denotes value of variable for the basic configuration.

TABLE 2

Constant C_p	D max/D_o	C_{D_o}	Max C_c	Max C_f	θ
1.2	.671	.500	.0189	.150	19°
1.5*	.671	.626	.0237	.185	19°
1.8	.672	.751	.0284	.220	19°
Linearly Varying C_p[1] $C_p(x_o)$					
1.500	.671	.626	.0237	.185	19°
1.882	.689	.707	.0268	.202	20°
2.268	.702	.785	.0299	.218	20°

[1] In the case labelled "Linearly varying C_p", C_p varies linearly in ϕ between $C_p(1) = 1.5$ (at vert) and $C_p(x_o)$ at the skirt.

which is exactly true only for $C_c(x_o)$, is also approximately true for the maximum value of C_c.

(vi) The fabric stress is greatest at or near the vent and decreases as we go toward the skirt. The exact location of the maximum fabric stress depends on E_f as well as the pressure distribution.

(vii) From Table 2 we see that for constant pressure distributions, changing the pressure scarcely affects the shape and causes merely proportional changes in the stresses. If the pressure increases linearly in ϕ from the vent to the skirt, all quantities are affected.

We shall comment on these results in the following Section.

5. DISCUSSION

The theory developed in this paper is apparently the first in which the shape and stresses are calculated simultaneously. To judge the theory we must of course compare it with experimental results. In making this comparison it is first necessary to understand clearly what the theory does.

If we are given a flat, circular canopy with known geometrical and physical properties (respectively embodied in R_i, R_o, L_o, G and E_f, E_c, and E_L), dropping vertically at known velocity V through air with known mass density, ρ, the analysis furnishes us with the relations between the pressure distribution on one hand and the shape, stresses and drag on the other. If the pressure distribution is known, we can solve these relations (by means of the computer program) to find the quantities of engineering interest. These quantities will depend in general upon the pressure distribution.

An ideal experimental check on the theory would require that simultaneous measurements of pressure distribution, stresses, shape and drag be made on a canopy that is dropping vertically. Conditions for such a test may be difficult or impossible to realize in practice, and it appears that no experiments yet made will permit such a complete check on the theory.

However, many experiments have been made that, while incomplete in some respect, give us the information for a partial check on the theory. For example, Berndt and Deweese[3] made measurements on a C-9 canopy in towed flight. Their results compare with the present calculation for the basic configuration as follows:

Measured	Calculated
$C_{D_o} = .65$	$C_{D_o} = .626$
$D_p/D_o = .648$	$D_p/D_o = .671$
$\Theta = 17^o$	$\Theta = 19^o$

Their measured shape is plotted in Figure 13. The general agreement is good although the theoretical shape is slightly wider and shallower than the experimental shape. We may conclude from this that the present theory is not grossly in error. However, it is necessary to remark that, if we had assumed a different pressure distribution in the calculations, we could have arrived at quite different values for C_{D_o}, as is evident from Table 2.

The Parachute Handbook[4] gives the general estimate

$$D_p/D_o \approx .7,$$

which compares reasonably well with the present calculations,

$D_p/D_o = .67$ for the cords

$= .73$ for the gore centerlines.

Moreover, the observed generality of this estimate tends to confirm the theory, which predicts that the shape is insensitive to changes in most of the parameters.

The Parachute Handbook[4] shows many experimental results in which C_D is seen to decrease with an increase in V. This does not agree, at first sight, with our results, Table 1, which show that C_{D_o} increases very slowly with an increase in V. The discrepancy is probably due to one or both of two causes:

(a) The canopy may not be descending vertically in the tests. The theory assumes vertical descent and may give inaccurate results if the canopy oscillates or glides laterally.

(b) The pressure distribution may change as the velocity changes. In particular, increasing velocity will cause increase of the tensile stresses and strains in the fabric, and this will lead to greater porosity of the fabric. The increasing porosity will permit increasing air flow from the high-pressure to the low-pressure side of the fabric. Thus the pressure difference will not increase as fast as the impact pressure, or, in other words, the pressure-difference coefficient, C_p, will decrease. This will cause C_{D_o} to decrease.

In general we may say that the present theory represents a first, admittedly somewhat crude, attempt to analyze parachutes without assuming the deformed shape. Clearly, several of the assumptions described in the Introduction are not very accurate, notably (ii), and (v), while (iv) is probably inaccurate near the maximum diameter. Nevertheless the results are good enough to suggest that the general procedure is a workable one which can be a starting point for future efforts.

It is perhaps also useful to point out that this theory represents a step in the direction of calculating the opening behavior of parachutes. For a major part of the difficulty in the opening problem consists of estimating the shape and forces of the inflated part of the canopy. The not-yet-inflated part of the canopy is relatively easily dealt with. The estimate of the shape and forces of the

inflated part of the canopy is much like that of a (smaller) completely open canopy. We may anticipate, therefore, that the present analysis, or one like it, will be an integral part of an analysis of opening behavior.

ACKNOWLEDGMENT

The author is indebted to the members of the Research and Advanced Projects Division in the Airdrop Engineering Laboratory at the U. S. Army Natick Laboratories, particularly Mr. E. J. Giebutowski, for both help and instruction during the course of this work.

REFERENCES

1. Heinrich, H. G. and Jamison, L. R., "Parachute Stress Analysis during Inflation and at Steady State", J. of Aircraft, Vol. 3, (1966), pp. 52-58.

2. Topping, A. D., Marketos, J. D. and Costakos, N. C., "A Study of Canopy Shapes and Stresses for Parachutes in Steady Descent", Wright Air Development Center TR 55 - 294, Goodyear Aircraft Corp. October 1955.

3. Berndt, R. J. and De Weese, J. H., "Filling Time Prediction Approach for Solid Cloth Type Parachute Canopies", AIAA Aerodynamic Deceleration Systems Conference, Houston, Texas 1966.

4. "Performance of and Design Criteria for Deployable Aerodynamic Decelerators", Air Force Systems Command Report No. ASD-TR-61-579, December 1963.

NOMENCLATURE

A_o, A_1, A_2, A_3	Constants in canopy pressure distribution
C_1, C_2	Constants in formulas for cosine function
C_{D_o}	Drag coefficient based on flat circular area
C_p	Coefficient of net pressure
C_c, C_f	Stress coefficients in cords, fabric
D_p, D_o	Diameters in opened and flat circular states
E_c, E_f, E_L	Elastic moduli of cords, fabric, load lines
f	$1+(N_c/E_c)$
G	Number of gores
J	Dimensionless load line length
L_o, L	Length of load lines in undeformed and deformed states
N_c, N_f	Tension force in cords, fabric
N_θ, N_n	Force resultants on cords in circumferential and normal directions
n_s, n_f,	Dimensionless force in cord, fabric
n_c	Dimensionless circumferential force resultant on cords
p	Net outward pressure on gore fabric
q	Dimensionless pressure
R	Radius of particle in flat circular state
R_i, R_o	Vent and skirt radii in flat circular state
r	Radius of cord in opened state
r_i, r_o	Vent and skirt radii in opened state
r_{AB}	Circumferential radius of curvature of gore

NOMENCLATURE (Cont'd)

s	Arc length of cord
S_1, S_2	Constants in formulas for sine function
U_f, U_i, U_L	Dimensionless elastic constants
V	Vertical velocity
D	Drag force
W	Dimensionless drag
x	Dimensionless radius in flat, circular state
x_o	Dimensionless skirt radius in flat circular state
y	Dimensionless radius in opened state
Z, Z_g	Axial cylindrical coordinate of cords and gore centerline
z, z_g	Dimensionless axial coordinate of cords and gore centerline
α	Included angle of gore
β	Edge angle of gore bulge
γ_s, γ_f, γ_L	Strains in cord, fabric, and load lines
δ	Depth in bulge
Δ	Dimensionless depth of bulge
θ	Angle between load line and axis
Λ	Load line length ratio = $L_o/D_o = JR_i/(2R_o)$
ρ	Mass density of air
σ'	Contact length between adjacent gores
σ	Dimensionless contact length between adjacent gores
ϕ	Angle between cord direction and horizontal
ϕ_o	ϕ at the skirt

Security Classification

DOCUMENT CONTROL DATA - R & D

(Security classification of title, body of abstract and indexing annotation must be entered when the overall report is classified)

1 ORIGINATING ACTIVITY (Corporate author) U.S. Army Natick Laboratories Natick, Mass 01760	2a. REPORT SECURITY CLASSIFICATION Unclassified 2b. GROUP

3 REPORT TITLE
Approximate Analysis of a Flat, Circular Parachute in Steady Descent

4 DESCRIPTIVE NOTES (Type of report and inclusive dates)

5 AUTHOR(S) (First name, middle initial, last name)
Edward W. Ross, Jr.

6 REPORT DATE December 1968	7a. TOTAL NO. OF PAGES 45	7b. NO OF REFS 4
8a. CONTRACT OR GRANT NO b. PROJECT NO 1F162203D195 c. d.	9a. ORIGINATOR'S REPORT NUMBER(S) 69-51-OSD 9b. OTHER REPORT NO(S) (Any other numbers that may be assigned this report)	

10. DISTRIBUTION STATEMENT
This document has been approved for public release and sale; its distribution is unlimited.

11 SUPPLEMENTARY NOTES	12 SPONSORING MILITARY ACTIVITY U.S. Army Natick Laboratories Natick, Mass 01760

13 ABSTRACT

A theory is presented for the stress analysis of a flat, circular parachute in steady, vertical descent. Unlike previous treatments of the problem, this theory does not assume that the shape is known. Instead the theory presents relations between the pressure distribution in the opened condition and the shape, drag and stresses in lines and fabric. The theory results in a non-linear third order system of ordinary differential equations with boundary conditions at both vent and skirt. This system was solved by a computer program based on the Runge-Kutta method of numerical integration. The results are in fairly good agreement with measurements on parachutes. The computer program can be used for studies of effects of design changes on shape, drag and stress, and the results of a small study of this sort are included.

DD FORM 1 NOV 68 1473 REPLACES DD FORM 1473, 1 JAN 64, WHICH IS OBSOLETE FOR ARMY USE.

Security Classification

KEY WORDS	LINK A		LINK B		LINK C	
	ROLE	WT	ROLE	WT	ROLE	WT
Stress analysis	8					
Parachutes	9		9			
Flat	0					
Circular	0					
Parachute descent	9		9			
Steady	0					
Vertical	0					
Pressure distribution	6.7					
Opened	0					
Shape	7.6		7			
Drag	7.6		7			
Stresses	7.6		7			
Parachute lines	7.6					
Parachute fabrics	7.6					
Design			6			
Revisions			6			
Computer programs			10			